A&A 488, 113–116 (2008)
DOI: 10.1051/0004-6361:200810141

Astronomy & Astrophysics

Supermassive black hole masses in type II active galactic nuclei with polarimetric broad emission lines

S.-Y. Zhang[1], W.-H. Bian[1,2], and K.-L. Huang[1]

[1] Department of Physics and Institute of Theoretical Physics, Nanjing Normal University, Nanjing 210097, PR China
e-mail: whbian@njnu.edu.cn
[2] Key Laboratory for Particle Astrophysics, Institute of High Energy Physics, Chinese Academy of Sciences, Beijing 100039, PR China

Received 6 May 2008 / Accepted 10 June 2008

ABSTRACT

Aims. Type II active galactic nuclei (AGNs) with polarimetric broad emission lines provided strong evidence for the orientation-based unified model for AGNs. We want to investigate whether the polarimetric broad emission lines in type II AGNs can be used to calculate their central supermassive black hole (SMBH) masses, like that for type I AGNs.

Methods. We collected 12 type II AGNs with polarimetric broad emission line widths from the literature, and calculated their central black hole masses from the polarimetric broad line widths and the isotropic [O III] luminosity. We also calculate the mass from stellar velocity dispersion, σ_*, with the $M_{\rm BH} - \sigma_*$ relation.

Results. We find that: (1) the black hole masses derived from the polarimetric broad line width is on average larger than that from the $M_{\rm BH} - \sigma_*$ relation by about 0.6 dex; (2) if these type II AGNs follow a $M_{\rm BH} - \sigma_*$ relation, we find that the random velocity cannot be omitted and is comparable to the broad-line regions (BLRs) Keplerian velocity. It is consistent with the scenery of large outflow from the accretion disk suggested by Yong et al.

Key words. galaxies: quasars: emission lines – galaxies: nuclei – black hole physics

1. Introduction

The standard paradigm for active galactic nuclei (AGNs) posits an accretion disk surrounding a central supermassive black hole (SMBH), along with other components, such as the broad-line regions (BLRs), narrow-line regions (NLRs), jet, and torus (e.g., Antonoucci 1993). The black hole mass ($M_{\rm BH}$) is an important parameter for us to understand the nuclear energy mechanics, the formation and evolution of SMBH, and galaxies (e.g., Rees 1984; Tremaine et al. 2002).

In the past decade, one of the most important advances in the study of AGNs is that the masses of SMBHs can be calculated by using the width of the broad emission lines from BLRs (e.g., Hβ, Hα, MgII, CIV) by the reverberation mapping method and several corresponding empirical relations (e.g., Kaspi et al. 2000; Bian & Zhao 2004; Greene & Ho 2006). In the orientation-based unified model for AGNs, the distinction between type I AGNs and type II AGNs depends upon whether the central engine and BLRs are viewed directly (type I) or are obscured by the circumnuclear torus (type II). Because of the absence of broad emission lines in the spectrum of type II AGNs, above methods for the mass calculation are only applicable to type I AGNs. The SMBH mass in the center of type II AGNs generally may be estimated by the $M_{\rm BH} - \sigma_*$ relation (e.g., Kauffmann et al. 2003; Bian & Gu 2007).

With spectro-polarimetric observation, some type II AGNs show hidden BLRs (HBLRs) and some do not (e.g., Antonucci & Miller 1985; Tran 1995). It is still not clear what kind of physical process is related to the presence of HBLRs in type II AGNs (e.g., Bian & Gu 2007). We calculate the SMBH mass in type II AGNs with HBLRs by using broad emission lines in their polarimetric spectrum as well as the $M_{\rm BH} - \sigma_*$ relation. In Sect. 2, we briefly introduce our sample. Section 3 introduces the methods to calculate the SMBH masses. Section 4 is the data analysis. Our results and discussions are given in Sect. 5. The last section is our conclusion. All of the cosmological calculations in this paper assume $H_0 = 70$ km s^{-1} Mpc^{-1}, $\Omega_M = 0.3$, $\Omega_\Lambda = 0.7$.

2. Sample

We collected a sample of 12 type II AGNs with HBLRs from the literature, which provide us with the hidden broad line width (Table 1). In this sample, there are 8 type II AGNs with redshifts $z < 0.05$ (Tran 1995), the rest are in the redshift range $0.3 < z < 0.8$, which are from Zakamska et al. (2007).

For Mrk 3 and Mrk 348, Tran (1995) used a sixth- or seventh-order polynomial to extract polarimetric broad line profiles for their high s/N. For the remaining objects in Tran (1995), multiple Gaussians are used to extract polarimetric broad line profiles for measuring the full widths at half-maximum (*FWHM*). For four objects in Zakamska et al. (2007), *FWHM* for polarimetric broad emission lines are obtained through Gaussian fits. These polarimetric broad emission lines are obvious because Zakamska et al. (2007) adopted a sensitivity limit of about 100 Å in equivalent width for these lines, which is larger than that for Hβ line in the composite quasar spectrum (46 Å; Vanden Berk et al. 2001).

3. Methods of calculating SMBH masses

3.1. Using the broad-line width to calculate the SMBH viral masses

Assuming that the gas in BLRs is virial in the gravitational field of the central SMBH, we can calculate the SMBH masses with the following formula (e.g., Kaspi et al. 2000; Kaspi et al. 2005):

$$M_{\rm BH} = \frac{R_{\rm BLR} v_{\rm BLR}^2}{G}, \quad (1)$$

Article published by EDP Sciences

where G is the gravitational constant, and $R_{\rm BLR}$ is the distance from BLRs clouds to the central black hole. This can be calculated from the monochromatic luminosity at 5100 Å (λL_λ(5100 Å)) by the empirical size-luminosity relation, that is (Kaspi et al. 2005):

$$R_{\rm BLR}^{\lambda L_\lambda(5100\ \text{Å})} = (22.3 \pm 2.1)\left(\frac{\lambda L_\lambda(5100\ \text{Å})}{10^{44}\ \text{erg s}^{-1}}\right)^{0.69\pm0.05}, \quad (2)$$

where $\upsilon_{\rm BLR}$ is the BLRs virial velocity, which can be traced by using *FWHM* of the broad Hβ line ($FWHM_{\rm H\beta}$) or H_γ line; that is:

$$\upsilon_{\rm BLR} = \sqrt{f} \times FWHM_{\rm H\beta}, \quad (3)$$

where f is the scaling factor. If BLRs cloud is disk-like with an inclination of θ (Wills & Browne 1986; Collin et al. 2006):

$$FWHM_{\rm H\beta} = 2(\upsilon_{\rm r}^2 + \upsilon_{\rm BLR}^2 \sin^2\theta)^{1/2}, \quad (4)$$

where $\upsilon_{\rm r}$ is the random isotropic component. If assuming $\upsilon_{\rm r} \ll \upsilon_{\rm BLR}$ and the random orbits of clouds in BLRs, then $f = 0.75$, i.e., $\sin^2\theta = 1/3$. Therefore, the formula (1) can be transformed into the following form:

$$M_{\rm BH} = 0.75 \times 4.35 \times 10^6 \left(\frac{FWHM_{\rm H\beta}}{10^3\ \text{km s}^{-1}}\right)^2 \left(\frac{\lambda L_\lambda(5100\ \text{Å})}{10^{44}\ \text{erg s}^{-1}}\right)^{0.69} M_\odot. \quad (5)$$

For type II AGNs, we could not obtain the intrinsic monochromatic luminosity at 5100 Å from their spectrum because of torus obscuration. The [O III]λ5007 luminosity, $L_{\rm [OIII]}$, coming from NLRs is not obscured and is isotropic. Kauffmann et al. (2003) have shown that the extinction-corrected $L_{\rm [OIII]}^{\rm cor}$ is a good indicator of AGN activity for type II AGNs. The unobscured monochromatic luminosity at 5100 Å is calculated by the following relation (e.g., Kaspi et al. 2000; Heckman et al. 2004; Netzer & Trakhtenbrot 2007):

$$L_{\rm bol} = 9[\lambda L_\lambda(5100\ \text{Å})] = 3500 L_{\rm [OIII]}^{\rm cor}. \quad (6)$$

3.2. $M_{BH} - \sigma_*$ relation

The second method for us to calculate the black hole masses is the relationship to the stellar velocity dispersion (σ_*) in their host galaxies (Tremaine et al. 2002):

$$M_{\rm BH}(\sigma_*) = 10^{8.13}\left(\frac{\sigma_*}{200\ \text{km s}^{-1}}\right)^{4.02}. \quad (7)$$

For 8 type II AGNs with redshifts $z < 0.05$, we obtained their stellar velocity dispersions from the literature (see Table 1). The other 4 type II AGNs in the redshift range $0.3 < z < 0.5$ are selected from the spectroscopic database of SDSS, their host galaxies light is too weak to directly measure the stellar velocity dispersion, σ_*. Because NLRs are primarily controlled by the host gravitational potential,the *FWHM* of the core/narrow [O III]λ5007 line after removing the asymmetric blue wing can be used to trace the stellar velocity dispersion for these 4 type II AGNs (Nelson & Whittle 1996; Greene & Ho 2005):

$$\sigma_* = FWHM_{\rm [OIII]}^{\rm core}/2.35. \quad (8)$$

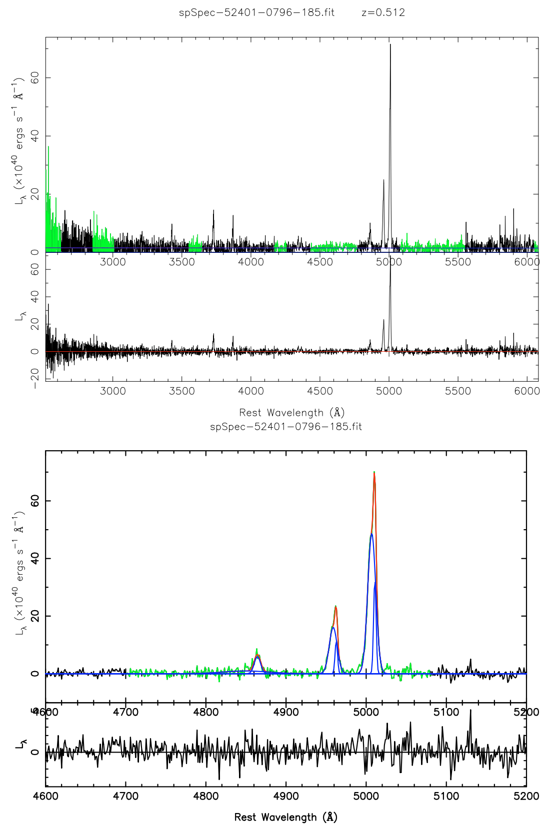

Fig. 1. Sample of SDSS spectrum measurement for J 1543+4395. In the top panel, the black curve is the observed spectrum, the green ranges are our fitting windows. In *the bottom panel*, the red line is the sum of all multi-Gaussians (blue curves), the green curve is our fitting range of the pure Hβ and [O III] emissions after the subtraction of the power-law continuum, the Balmer continuum, and Fe multiples.

4. Data analysis

For 4 type II AGNs with redshifts $0.3 < z < 0.5$, we downloaded their spectrum from the SDSS(the Sloan Dgital Sky Survey) spectroscopic database and used following steps to do the SDSS spectral measurements, which has been used for SDSS type I AGNs. (1) First, we estimate the Galactic extinction in observed spectra by using the extinction law of Cardelli et al. (1989, IR band) and O'Donnell (1994, optical band), then the spectra are transformed into the rest frame defined by the redshifts given in their FITS headers. (2) The FeII template is from NLS1 I ZW1 model, the Balmer continuum are calculated following Grandi (1982). The best subtraction of the FeII, power-law and Balmer continuum is found when χ^2 minimized in the fitting windows: 3550–3645, 4170–4260, 4430–4770, 5080–5550, 6050–6220, 6890–7010 Å. Since they are the spectra of type II AGNs, the FeII line and Balmer continuum could be neglected, the power-law continuum seems flat (see a sample fit in the a panel of Fig. 1). (3) Two sets of two-Gaussian are used to model [O III]$\lambda\lambda$4959, 6007 lines. We take the same line width for each component, and fix the flux ratio of [O III]λ4959 to [O III]λ5007 to be 1:3. Two-Gaussian profile is used to model Hβ line. (see the b panel of Fig. 1). From above spectral measurement, we obtain the *FWHM* of the narrow/core [O III] line, as well as the total [O III] luminosity (see Table 1).

Table 1. The properties for 12 type II AGNs with HBLRs.

name	z	$\log(L_{[O\,III]})$ erg s^{-1}	$FWHM_{[O\,III]}$ km s^{-1}	σ_* km s^{-1}	$FWHM_{H\beta}$ km s^{-1}	$\log(M_{H\beta}/M_\odot)$	$\log(M_{\sigma_*}/M_\odot)$	Ref.
(1)	(2)	(3)	(4)	(5)	(6)	(7)	(8)	(9)
NGC1068	0.004	42.645[a]	–	128	3030	7.88	7.35	1, 1, 2
NGC7212	0.027	42.636[a]	–	137	5420	8.37	7.47	1, 1, 2
NGC7674	0.029	42.495[a]	–	144	2830	7.82	7.56	1, 1, 2
Mrk3	0.014	43.221[a]	–	269	6000	9.17	8.65	1, 1, 2
Mrk348	0.015	41.912[a]	–	185	9350	8.17	7.99	1, 1, 2
Mrk463E	0.050	42.785[a]	–	137	2770	7.81	7.88	1, 1, 2
Mrk477	0.038	43.543[a]	–	117	4130	8.84	7.19	1, 1, 2
Mrk1210	0.013	42.195[a]	–	77	3080	7.90	6.46	1, 1, 2
J0842+3625	0.561	43.601[b]	303.76	129.30[c]	4900(H_γ)	8.99	7.37	3, 3, 4
J1039+6430	0.402	42.901[b]	385.75	164.15[c]	3070	7.89	7.79	3, 3, 4
J1543+4935	0.512	42.789[b]	709.72	302.01[c]	4300	8.19	8.84	3, 3, 4
J1641+3858	0.596	43.474[b]	395.72	168.39[c]	3200(H_γ)	8.62	7.83	3, 3, 4

Notes. – Col. (1), name; Col. (2), redshift; Col. 3, the [O III] luminosity; Col. (4), *FWHM* of the narrow [O III] line; Col. (5), stellar velocity dispersion; Col. (6), *FWHM* of Hβ from HBLRs; Col. (7), SMBH masses derived from the polarimetric broad line; Col. (8), SMBH masses derived from the $M_{BH} - \sigma_*$ relation. Col. (9), reference for Cols. (3,5,6): (1) Bian & Gu (2007); (2) Tran (1995); (3) this work; (4) Zakamska et al. (2005). [a]: the intrinsic extinction-corrected [O III] luminosity; [b]: the intrinsic extinction-uncorrected [O III] luminosity; [c]: the stellar velocity dispersion is derived from the *FWHM* of the narrow/core [O III].

5. Results and discussion

5.1. Results

In Table 1, we presented our results. We used formulas (5) and (6) to calculate the virial SMBHs masses, which is listed in Col. (7) in Table 1. By the $M_{BH} - \sigma_*$ relation, we used formulas (7) and (8) to calculate the SMBHs masses from σ_*, which is listed in Col. (8) in Table 1. We find that, except two objects, Mrk463E and SDSS J1543+4395 (see Fig. 2), the black hole masses from the broad line width in spectro-polarimetric observations are larger than that from the $M_{BH} - \sigma_*$ relation. The mass from the polarimetric broad line width is on average larger than that from $M_{BH} - \sigma_*$ relation by about 0.6 dex.

For SDSS J1543+4935, the mass from the $M_{BH} - \sigma_*$ relation is larger that from the polarimetric broad line width by 0.65 dex (see Table 1). We note that, with respect to other three objects, it is difficult to define its narrow/core component from the [O III]λ5007 emission line profile (see Figs. 1 and 3). Here we used the *FWHM* of the [O III]λ5007 emission line component with larger flux as the tracer of the σ_*. The dynamics of NLRs clouds for SDSS J1543+4935 is probably special. If we neglect SDSS J1543+4395, we find that the average mass difference would be larger, from 0.6 dex to 0.7 dex.

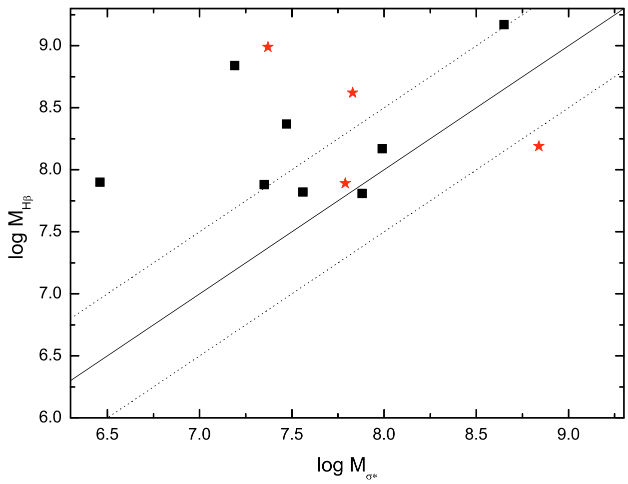

Fig. 2. log $M_{H\beta}$ vs. log M_{σ_*}. $M_{H\beta}$ is from the polarimetric broad-line width, M_{σ_*} is calculated from the $M_{BH} - \sigma_*$. Black square denotes the type II AGNs with redshifts $z < 0.05$, red star denotes the type AGNs with $0.3 < z < 0.8$. The solid line denotes 1:1 and the dotted lines are $y = x \pm 0.5$.

5.2. Discussion

The uncertainties in the black hole masses estimated by the $M_{BH} - \sigma_*$ relation depend upon the uncertainties in the stellar dispersion and the $M_{BH} - \sigma_*$ relation. For the typical uncertainty of 20 km s^{-1} for $\sigma_* = 200$ km s^{-1}, the error of log σ_* would be about 0.05 dex, corresponding to 0.2 dex for log M_{bh}. Considering the error of 0.3 dex form the $M_{bh} - \sigma_*$ relation (Tremaine et al. 2002), the error of log M_{bh} is about 0.4.

For the mass estimated by the polarimetric broad-line width, the accuracy of the results depend on the *FWHM* measurement of the broad Hβ, the unobscured 5100 Å luminosity, the BLRS dynamics, and the empirical size-luminosity relation. The usage of size-luminosity relation of Bentz et al. (2006) is almost the same as that of Kaspi et al. (2006) for masses larger than $10^7\,M_\odot$. It is generally believed that the uncertainty from this method is about 0.5 dex (e.g., Bian & Gu 2007). The spectral resolution in the polarimetric observation is about 8 Å for objects studied by Tran (1995) and 19 Å for objects studied by Zakamaska et al. (2005). For our sample, we find that the instrumental correction in *FWHM* will lead to a mass uncertainty of less than 0.1 dex.

For the 12 type II AGNs with polarimetric broad emission lines, we find that the M_{BH} derived from the broad-line width is generally larger than that from the $M_{BH} - \sigma_*$ relation, with an average of 0.6 dex higher. The intrinsic extinction-uncorrected [O III] luminosity for 4 SDSS objects is the lower limit. Considering the intrinsic correction, the mass derived from polarimetric broad-line width would be larger. Because the mass from the broad-line width is $\propto FWHM^2_{H\beta}\,\lambda L_\lambda(5100\,\text{Å})^{0.69}$, the larger mass derived from polarimetric broad-line width is mainly due to the overestimate of virial velocity of SMBHs estimated from Hβ *FWHM* versus formula (4). It is possible that the profile from HBLR is broadened in the polarimetric observation.

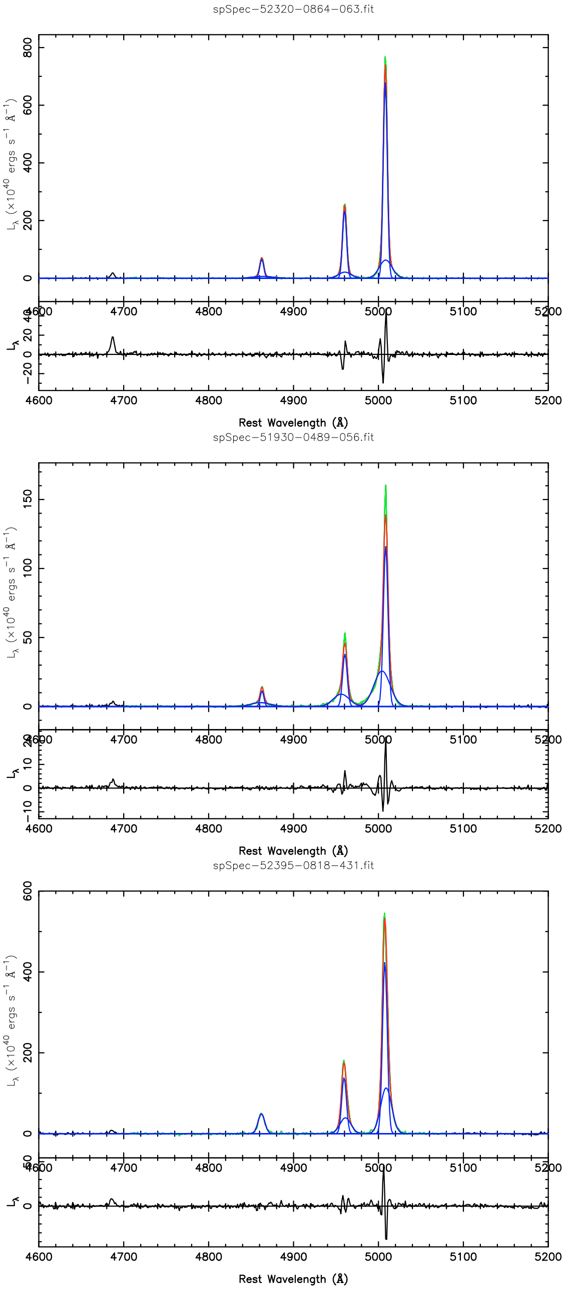

Fig. 3. The [O III] double line fitting for SDSS J0842+3625, SDSS J1039+6430 and SDSS J1641+3858 (from *top to bottom*).

There exists other nonvirial broaden effect for the polarimetric broad line. If it is not the case, considering the formula (4), $FWHM_{\mathrm{H}\beta} = 2(v_{\mathrm{r}}^2 + v_{\mathrm{BLR}}^2 \sin^2\theta)^{1/2}$, it is possible that the random isotropic velocity cannot be neglected. Therefore, there exists a strong random isotropic velocity in BLRs, such as outflows in HBLRs. The speeds of outflow expanding away from the accretion disk may be comparable to the virial velocity of the clouds in HBLR (Yong et al. 2007), the profile from HBLR may be broaden due to the scatter in the outflow. Considering the random orbits of BLRs clouds, $\sin^2\theta = 1/3$, and $v_{\mathrm{r}} \sim v_{\mathrm{BLR}}$, the mass from the polarimetric broad lines *FWHM* would decreased by 0.6 dex, which will make the mass from polarimetric broad lines *FWHM* consistent with that from the $M_{\mathrm{BH}} - \sigma_*$ relation.

For type II AGNs, the central engine and BLRs are not viewed directly due to obscuration by the circum-nuclear torus. They are seen at a large torus inclination to the line of sight. We are not sure whether BLRs are coplanar with the torus. If they are coplanar, type II AGNs are seen at a large BLRs inclination to the line of sight. By $\sin^2\theta = 1$, i.e., "*edge − on*", the mass from equation (5) would decreased by 0.48 dex respect to that for $\sin^2\theta = 1/3$, which is still on average larger than that from $M_{\mathrm{BH}} - \sigma_*$ relation. When the random isotropic velocity cannot be neglected, e.g., $v_{\mathrm{r}} \sim v_{\mathrm{BLR}}$, the "*edge − on*" BLRs geometry would lead the mass from Eq. (5) decreased by 0.18 dex with respect to the random BLRs clouds. In this case, the inclination is not the dominant source of the larger SMBH masses deviation between the mass from the width of polarimetric broad emission lines and that from the $M_{\mathrm{BH}}-\sigma_*$ relation, while the large random velocity is the dominant source (see also Collin et al. 2006).

6. Conclusion

The central SMBHs masses for 12 type II AGNs with polarimetric broad lines are estimated from the broad line *FWHM* and the [O III]luminosity, as well as the $M_{\mathrm{BH}} - \sigma_*$ relation. We find that: (1) the SMBH masses derived from the width of polarimetric broad emission lines is averagely larger than that from the $M_{\mathrm{BH}} - \sigma_*$ relation by about 0.6 dex; (2) if these type II AGNs follow $M_{\mathrm{BH}} - \sigma_*$ relation, our result suggests that the random velocity cannot be omitted and is comparable with the BLRs Keplerian velocity. It is consistent with the scenery of larger outflow from the accretion disk suggested by Yong et al. (2007).

Acknowledgements. We thank the anonymous referee for helpful suggestions. We thank discussions among people in IHEP AGN group. This work has been supported by the NSFC (Nos. 10733010, 10473005, 10325313, 10733010, 10521001 and KJCX2-YW-T03.), the Science-Technology Key Foundation from Education Department of P. R. China (No. 206053), and the China Postdoctoral Science Foundation (No. 20060400502).

References

Antonucci, R. 1993, ARA&A, 31, 473
Antonucci, R., & Miller, J. S. 1985, ApJ, 297, 621
Bian W., & Zhao Y. 2004, MNRAS, 347, 607
Bian W., & Gu Q. 2007, ApJ, 657, 159
Collin S. 2006, A&A, 456, 75
Cardelli, J. A.,Clayton, G. C., &Mathis, J. S. 1989, ApJ, 345, 245
Goosmann R. W., & Gaskell C. M. 2007, A&A, 465, 129
Grandi, S. A. 1982, ApJ, 155, 25
Greene, J. E., & Ho, L. C. 2005, ApJ, 627, 721
Greene, J. E., & Ho, L. C. 2006, ApJ, 641, 117
Heckman, T. M. 2004, ApJ, 613, 109
Kaspi, S., Smith, P. S., Netzer, H., et al. 2000, ApJ, 533, 631
Kaspi, S., Maoz, D., Netzer, H., et al. 2005, ApJ, 629, 61
Kauffmann, G., Heckman, T. M., Tremonti, C., et al. 2003, MNRAS, 346, 1055
Mclure, R. J., & Jarvis, M. J. 2002, MNRAS, 337, 109
Nelson, C. H., & Whittle, M. 1996, ApJS, 99, 67
Netzer, H., & Trakhtenbrot, B. 2007, ApJ, 654, 754
O'Donnell, & James, E. 1994, ApJ, 422, 158
Rees, M. J. 1984, ARA&A, 22, 471
Richards, G. T., Lacy, M., Storrie-Lombardi, L. J., et al. 2006, ApJS, 166, 470
Yong, S., Axon, D. J., Robinson, A., et al. 2007, Nature, 450,74
Tremaine, S., Gebhardt, K., Bender, R., et al. 2002, ApJ, 574, 740
Tran, H. D. 1995, ApJ, 440, 565
Vanden Berk, D. E., Daniel E., Richards, G. T.; Bauer, A., et al. 2001, AJ, 122, 549
Wills, B. J., & Browne, I. W. A. 1986, ApJ, 302, 56
Zakamaska, N. L., Schmidt, G. D., Smith, P. S., et al. 2005, AJ, 129, 1212